

PAN/PI Functional Double-layer Coating for Dendrite-Free Lithium Metal Anodes

Fei Shen^{1, a}, Kaiming Wang^{1, a}, Yuting Yin¹, Le Shi¹, Dingyuan Zeng¹, Xiaogang Han^{1, 2*}

¹State Key Laboratory of Electrical Insulation and Power Equipment, School of Electrical Engineering, Xi'an Jiaotong University, Xi'an 710049, Shaanxi, China

²Key Laboratory of Smart Grid of Shaanxi Province, Xi'an, Shaanxi 710049, China

^aThe authors contribute equally to this paper

*Correspondence to: xiaogang.han@xjtu.edu.cn

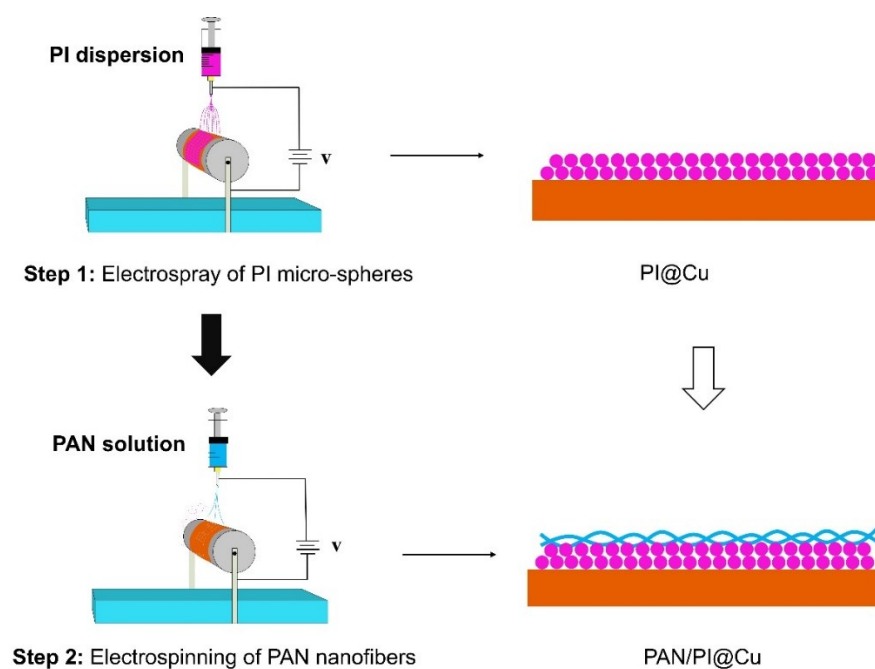


Fig. S1 The preparation process of PAN/PI@Cu.

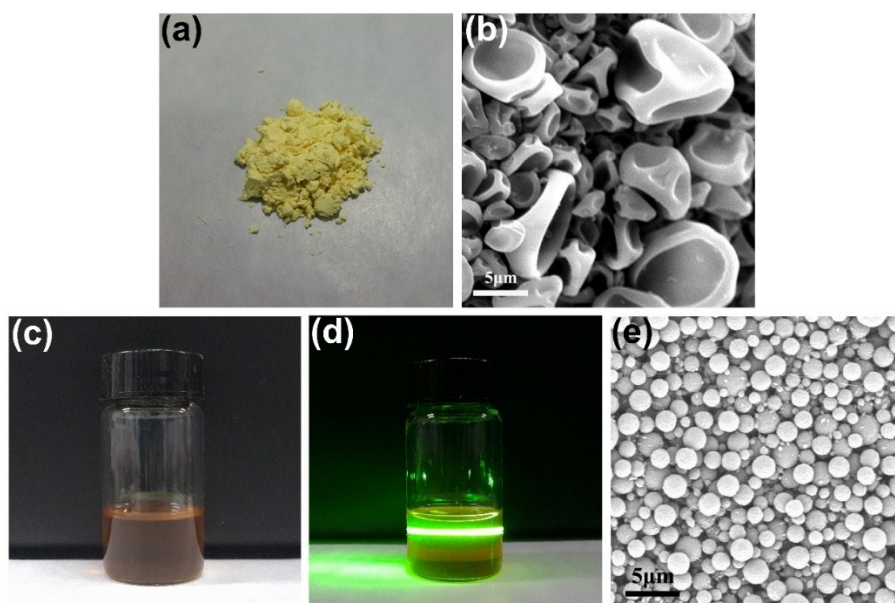


Fig. S2 (a) Optical photograph and (b) SEM image of raw PI material, (c, d) optical photograph of PI dispersion and (e) SEM image of PI after electrospray.

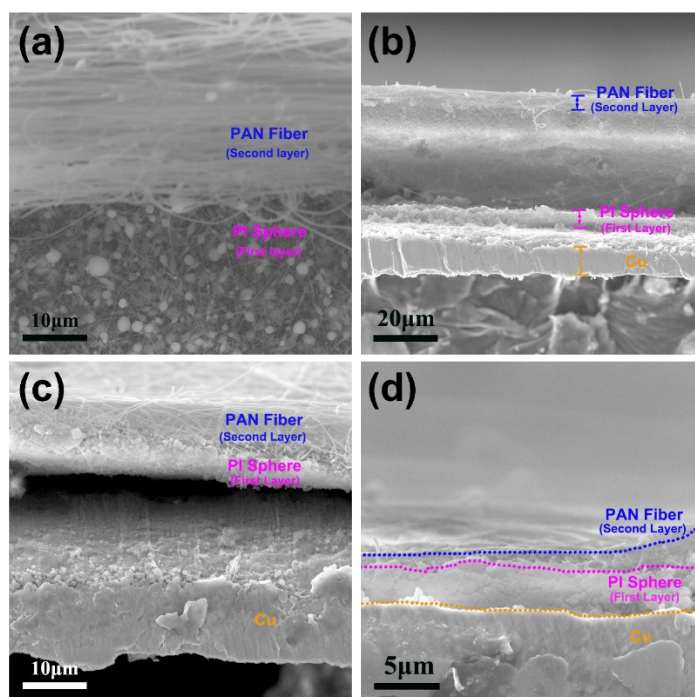


Fig. S3 SEM images to reveal two coating layers in PAN/PI@Cu. (a) top-view and (b-d) cross-section.

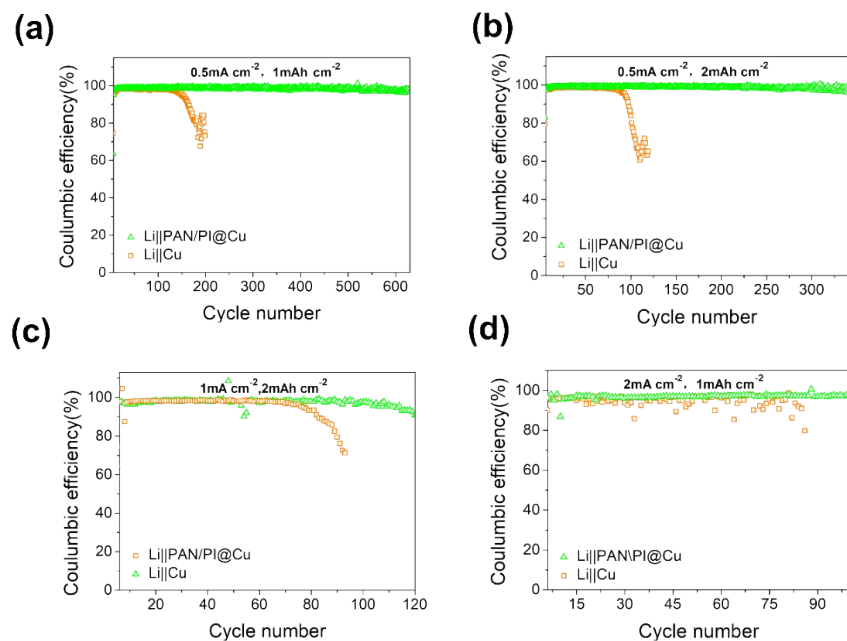


Fig. S4 Comparison of Coulombic efficiency of Li||Cu and Li||PAN/PI@Cu at various current densities with different deposition capacities. (a) 0.5 mA cm⁻², 1 mAh cm⁻², (b) 0.5 mA cm⁻², 2 mAh cm⁻², (c) 1 mA cm⁻², 2 mAh cm⁻² and (d) 2 mA cm⁻², 1 mAh cm⁻².

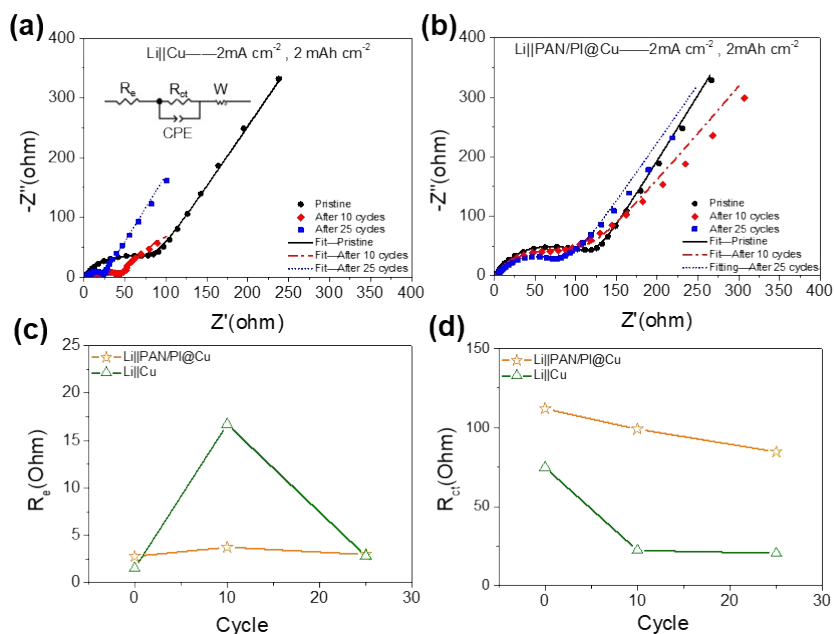


Fig. S5 Impedance spectroscopy of (a) Li||Cu, (b) Li||PAN/PI@Cu and (c-d) corresponding equivalent resistances with different galvanostatic cycles.

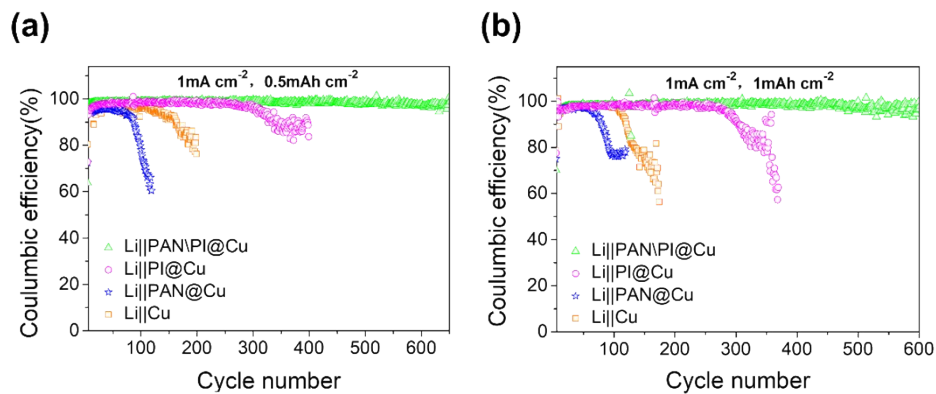


Fig. S6 Coulombic efficiencies of cells at a current density of 1 mA cm^{-2} with deposition capacities of (a) 0.5 mAh cm^{-2} and (b) 1 mAh cm^{-2} .

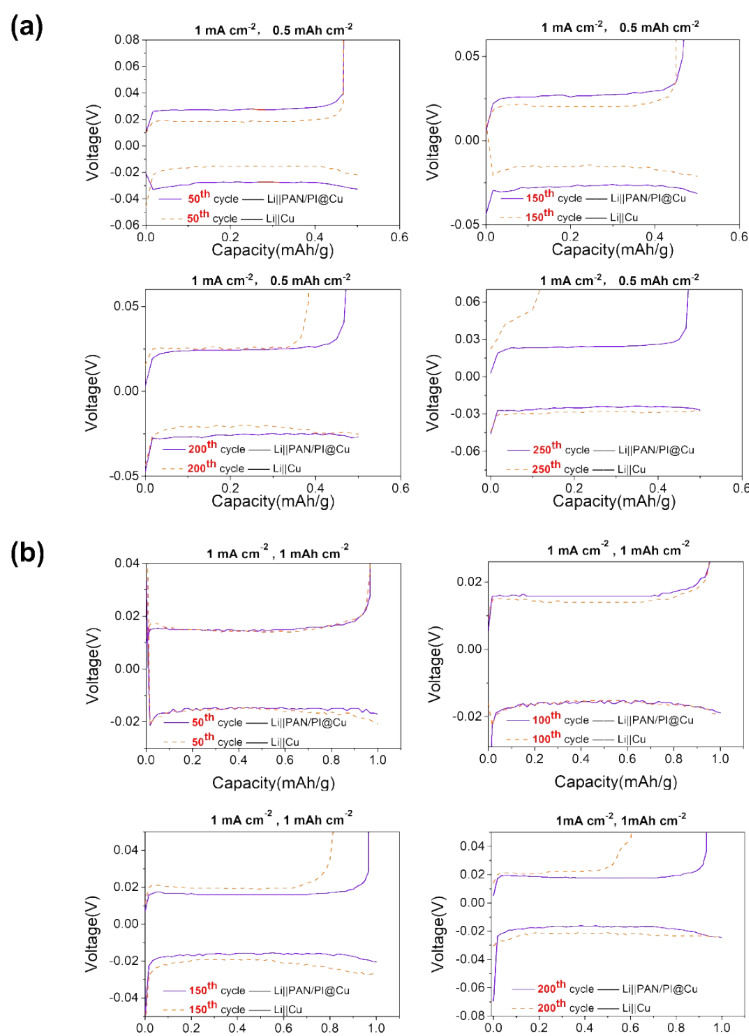


Fig. S7 Comparison of ΔV s between plating and stripping plateaus of Li||Cu and Li||PAN/PI@Cu during different cycles at a current density of 1 mA cm^{-2} with various deposition capacities of (a) 0.5 mAh cm^{-2} and (b) 1.0 mAh cm^{-2} .

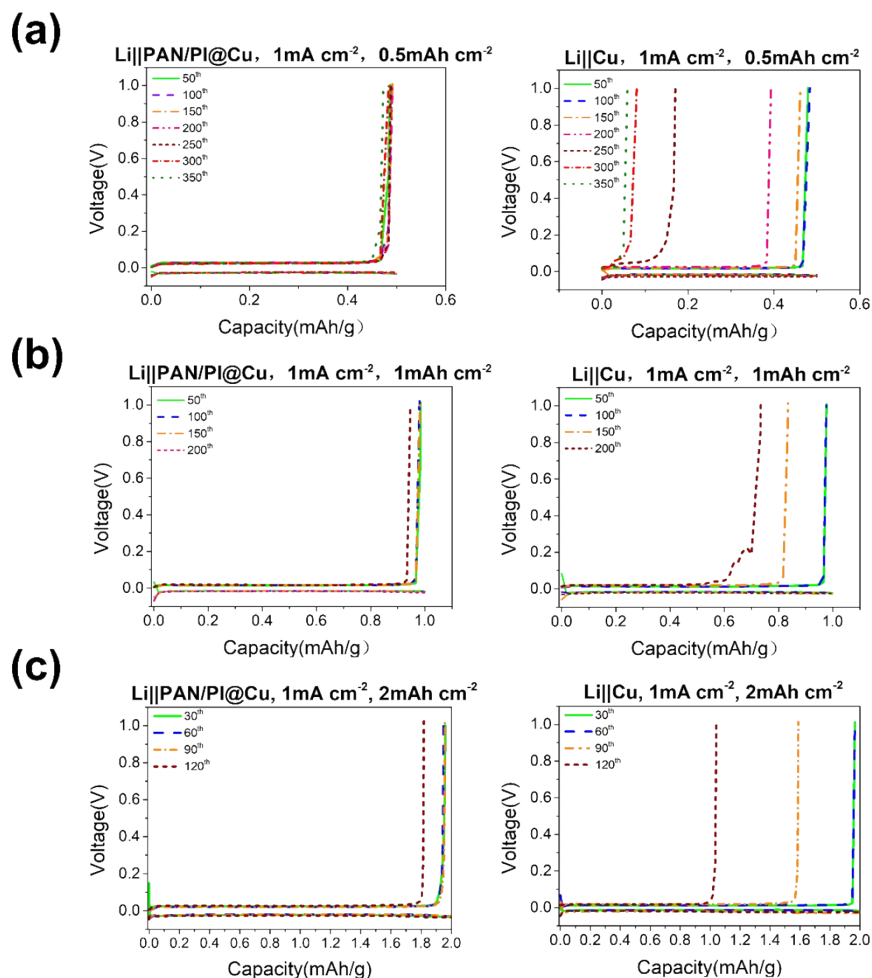


Fig. S8 Comparison of the voltage profiles of the Li plating/stripping processes of Li||Cu and Li||PAN/PI@Cu at a current density of 1mA cm^{-2} with deposition capacities of (a) 0.5mAh cm^{-2} , (b) 1mAh cm^{-2} and (c) 2mAh cm^{-2} .

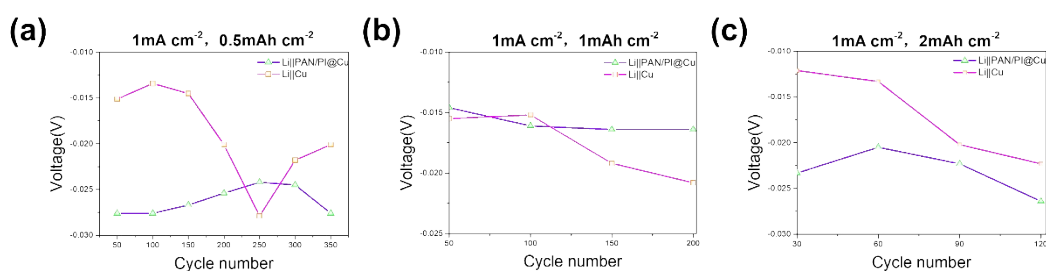


Fig. S9 Comparison of the battery voltages at the same discharging time (depositing same amount of Li) in different cycles.

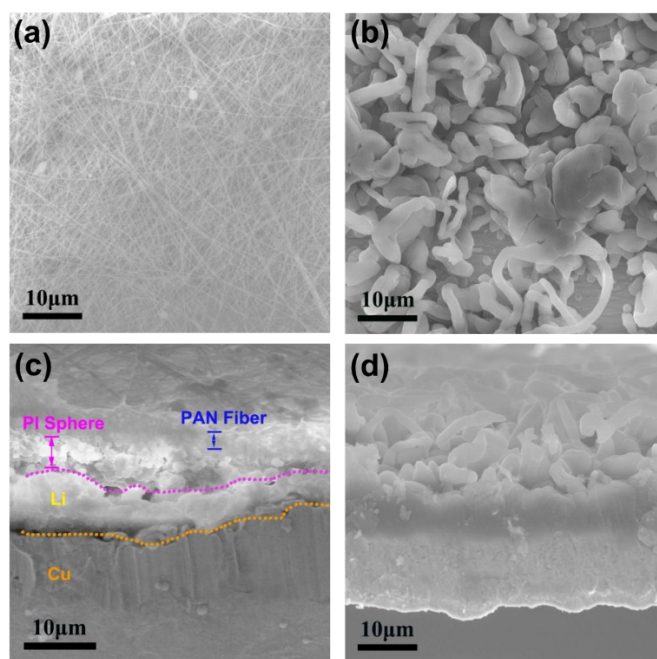


Fig. S10 Comparison of SEM images of the deposited Li metal on bare Cu and PAN/PI@Cu. Top-view SEM images of (a) PAN/PI@Cu and (b) bare Cu; Cross-section SEM image of (c) PAN/PI@Cu and (d) bare Cu. The deposition capacity is 1 mAh cm^{-2} .

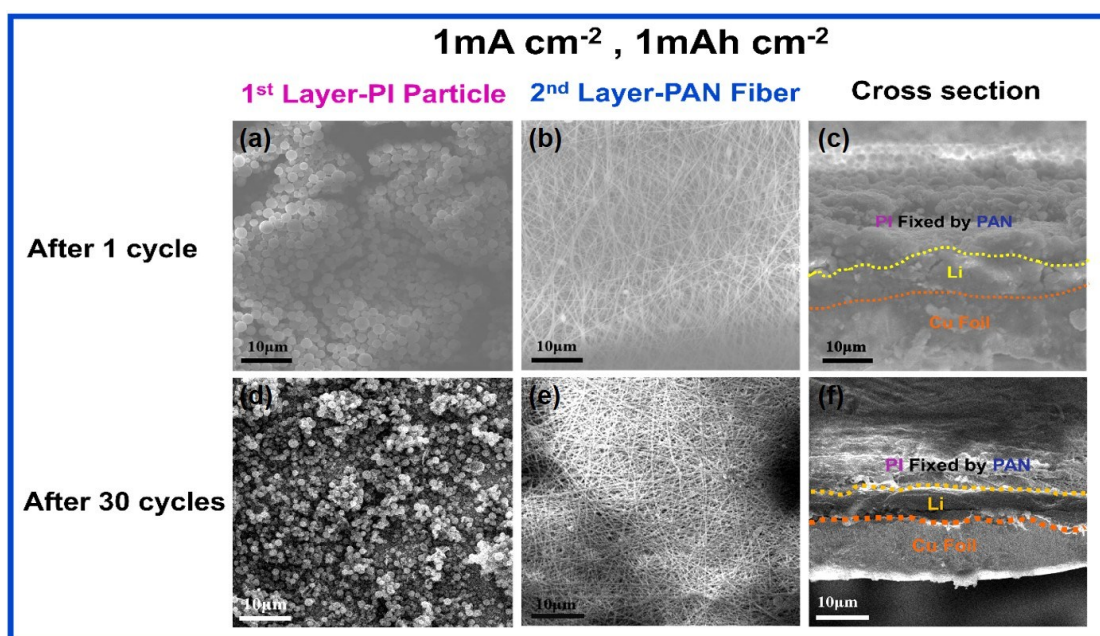


Fig. S11 SEM images of Li deposits at a current density of 1 mA cm^{-2} with a deposition capacity of 1 mA cm^{-2} after (a-c) 1 cycle and (d-f) 30 cycles.

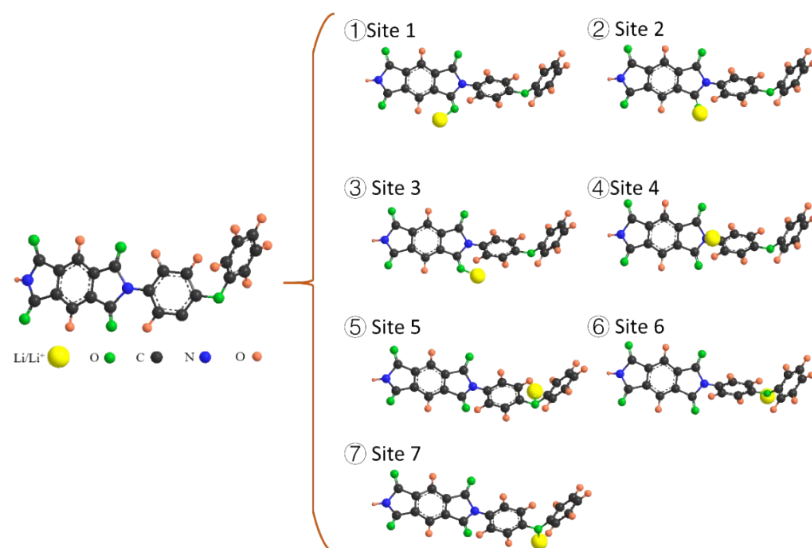


Fig. S12 The adsorption model of Li atom and Li ion at PI.

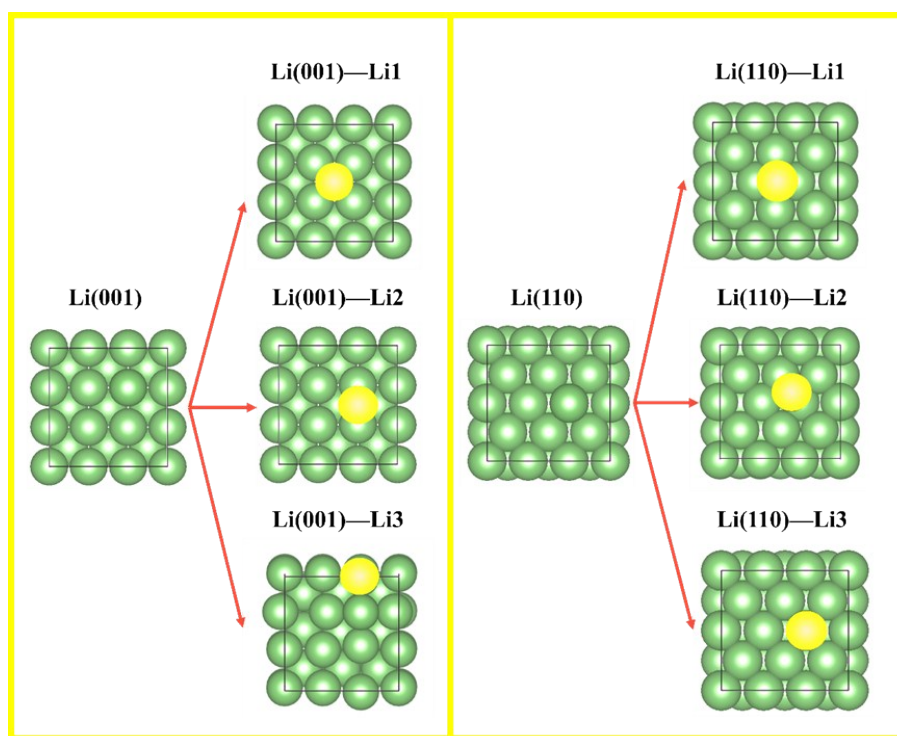


Fig.S13 The adsorption model of Li atom at deposited Li metal.

Table R1 Atomic Absorption Spectroscopy result

Analyte	Relative absorbance	Concentration(mg/L)	Standard deviation(mg/L)
	.0915	0.624	
Li 670.78	.0931	0.635	
	.0930	0.635	
Average value	.0925	0.631	0.0060

For atomic absorption spectroscopy sample preparation, 1g PI powder was added to 10 mL electrolyte (1 M LiTFSI in DOL/DME) and stirred until dispersed homogeneously. Then, the above dispersion was centrifuged. PI sediment was transferred into ethanol, sonicated and filtered for 4 times at least to remove excess Li ions and leave only the adsorbed Li ions. After that, the PI powder was added into deionized water, stirred and sonicated for hours to desorb the adsorbed Li ions into the water solvent. Then the water dispersion was centrifuged and the supernatant was used for AAS test.